Received: 13 June 2023 | Revised: 4 October 2023 | Accepted: 19 October 2023

DOI: 10.1002/cac2.12500

CANCER COMMUNICATIONS Open Access

LETTER TO THE EDITOR

Mitochondria-targeted atovaquone promotes anti-lung cancer immunity by reshaping tumor microenvironment and enhancing energy metabolism of anti-tumor immune cells

Dear Editor,

Atovaquone (ATO), a mitochondrial inhibitor, has anti-cancer effects [1]. Based on ATO, we developed mitochondria-targeted atovaquone (Mito-ATO) that had even stronger anti-tumor efficacy than ATO [2]. We synthesized Mito-ATO by attaching the bulky triphenylphosphonium (TPP) group to ATO via a ten-carbon alkyl chain (Supplementary file of methods; Supplementary Figure S1). To assess the effects of Mito-ATO on tumor microenvironment, we conducted single-cell RNA-sequencing (scRNA-seq) on treated immune cells from mice having lung tumors either treated with or without Mito-ATO. Seurat was used for clustering and annotation of $CD45^+$ immune cells [3]. The detected lymphoid cell populations were $CD8^+$ T cells, $CD4^+$ T cells, regulatory T cells (Tregs), gamma-delta T (Tgd) cells, B cells, and natural killer (NK) cells; and the myeloid cells identified were macrophages, neutrophils, plasmacytoid dendritic cells (pDCs), conventional dendritic cells (cDCs) and mast cells (Figure 1A-C). Clustering of $CD4^+$ T cells into seven subpopulations, the separation of neutrophils and granulocytic myeloid-derived suppressor cells (G-MDSCs), and the division of macrophages into M1 and M2 subtypes were described in our previous publication [2]. In this study, we further divided $CD8^+$ T cells into four subpopulations, i.e., exhausted $CD8^+$ T (CD8T_Exhausted) cells, memory like $CD8^+$ T (CD8T_MemoryLike) cells, effector memory like $CD8^+$ T (CD8T_EffectorMemory) cells and naive $CD8^+$ T (CD8T_Naive) cells, using the tumor-infiltrating $CD8^+$ lymphocyte state predictor (TILPRED) method [4] (Figure 1D-E). Probability scores computed with TILPRED could discriminate CD8T_Exhausted from CD8T_MemoryLike cells despite overlap between the two subsets on UMAP representation (Supplementary Figure S2). Mito-ATO treatment significantly decreased the proportion of the CD8T_Exhausted cells (7.3% vs. 32.5%, $P < 0.001$) but increased the proportion of anti-tumor CD8T_EffectorMemory cells as compared with vehicle treatment (37.3% vs. 11.9%, $P < 0.001$) (Figure 1F). In comparison, the percentages of $CD8^+$ T cells out of total T cells were not different between the two groups (Supplementary Table S1). For validation, we verified that Mito-ATO treatment induced changes in $CD8^+$ T cell repartition by conducting flow cytometry. Mito-ATO treatment significantly increased the percentage of cytotoxic tumor necrosis factor-alpha $(TNF\text{-}\alpha)^+CD8^+$ T cells and decreased the percentage of programmed cell death protein-1 $(PD\text{-}1)^+$ T cell immunoglobulin and mucin domain-containing protein 3 $(TIM3)^+CD8^+$ T cells (Supplementary Figure S3). These matched the scRNA-seq results. We also observed a slight trend toward the upregulation of genes involved in $CD8^+$ T cell recruitment: Ccl25, Ccr7, Cxcl10, Cxcr3, Icam1, and S1pr1 (Supplementary Figure S4).

List of abbreviations: Aco1, aconitase 1; Aco2, aconitase 2; ATO, atovaquone; CD4IL2RAHI, IL2RA-high $CD4^+$ Treg; CD4IL2RALO, IL2RA-low $CD4^+$ Treg; CD4T_Cytotoxic, cytotoxic $CD4^+$ T cells; CD4T_Exhausted, exhausted $CD4^+$ T cells; CD8T_EffectorMemory, effector memory like $CD8^+$ T cells; CD8T_Exhausted, exhausted $CD8^+$ T cells; CD8T_MemoryLike, memory like $CD8^+$ T cells; CD8T_Naive, naive $CD8^+$ T cells; cDC, conventional dendritic cells; FDR, false discovery rate; Glud1, glutamate dehydrogenase 1; G-MDSC, granulocytic myeloid-derived suppressor cells; Got1, glutamic-oxaloacetic transaminase 1; Idh3a, isocitrate dehydrogenase 3 alpha; Idh3b, isocitrate dehydrogenase 3 beta; Idh3g, isocitrate dehydrogenase 3 gamma; Ldha, lactate dehydrogenase A; Mdh1, malate dehydrogenase 1; Mdh2, malate dehydrogenase 2; Mito-ATO, mitochondria-targeted atovaquone; Mpc2, mitochondrial pyruvate carrier 2; NES, normalized enrichment score; NK, natural killer cells; OXPHOS, oxidative phosphorylation; pDC, plasmacytoid dendritic cells; Pkm, pyruvate kinase; ROS, reactive oxygen species; TCA, tricarboxylic acid; Tgd, gammadelta T cells; TILPRED, tumor-infiltrating $CD8^+$ lymphocytes states predictor; TPP, triphenylphosphonium; Tregs, regulatory T cells.

CANCER COMMUNICATIONS Open Access

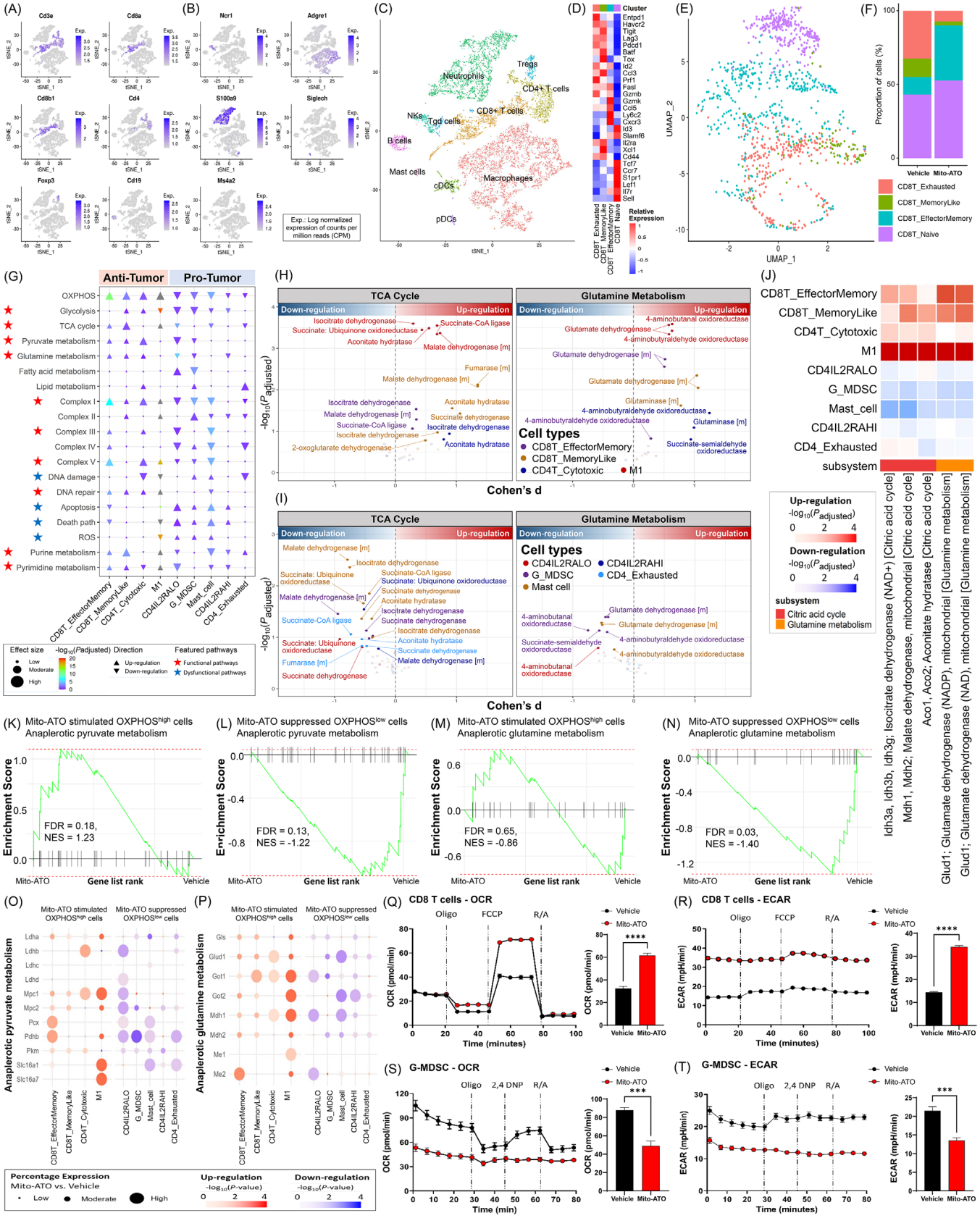

FIGURE 1 Single-cell RNAseq analysis of immune cells from mice lung tumors to identify mechanisms of Mito-ATO's anti-tumor function. (A) The expression of the marker genes for the T and B lymphocytes; (B) The expression of the marker genes for the NK cells, macrophages, neutrophils, pDC, cDC and mast cells; (C) The annotation of all the sequenced immune cells to the above lymphocytes and

Mito-ATO treatment significantly up-regulated oxidative phosphorylation (OXPHOS) activity in four anti-tumor immune cell populations, i.e., CD8T_EffectorMemory cells, CD8T_MemoryLike cells, cytotoxic $CD4^+$ T cells (CD4T_Cytotoxic), and M1 macrophage cells (Figure 1G). Particularly, the upregulated genes after Mito-ATO treatment were significantly enriched for T cell differentiation (Supplementary Figure S5), suggesting that Mito-ATO treatment may induce $CD8^+$ T cell differentiation. In contrast, Mito-ATO treatment significantly down-regulated OXPHOS activity in five pro-tumor immune cell populations, i.e., interleukin-2 receptor subunit alpha (IL2RA)-low $CD4^+$ (CD4IL2RALO) Tregs, G-MDSCs, mast cells, IL2RA-high $CD4^+$ (CD4IL2RAHI) Tregs, and exhausted $CD4^+$ T cells (CD4T_Exhausted) (Figure 1G). The two types of Treg cells were named following the previous practice [2, 5]. Ten metabolic pathways activity changes were similar to OXPHOS activity changes by Mito-ATO treatment in the above immune cell populations. These pathways were glycolysis, the tricarboxylic acid (TCA) cycle, pyruvate metabolism, glutamine metabolism, Complex I, Complex III, Complex V, DNA repair, purine metabolism and pyrimidine metabolism (Figure 1G). The changes of four cell death-related pathways, i.e., DNA damage, apoptosis, cell death, and reactive oxygen species (ROS) pathways, were negatively correlated with OXPHOS activity changes by Mito-ATO treatment (Figure 1G). These suggested that Mito-ATO enhances energy metabolism and suppresses cell death in anti-tumor immune cells while inhibiting energy metabolism and promoting cell death in pro-tumor immune cells.

Compass metabolism analysis [6] showed similar results (Supplementary Figures S6-S14) . The key metabolic reactions of the TCA cycle and glutamine metabolism were up-regulated in the anti-tumor immune cell populations but down-regulated in the pro-tumor immune cell populations (Figure 1H-I). We identified key metabolic reactions differentially regulated by Mito-ATO across anti-tumor and pro-tumor immune cells, including aconitase 1 (Aco1)/Aco2, malate dehydrogenase 1 (Mdh1)/Mdh2, isocitrate dehydrogenase 3 alpha (Idh3a)/Idh3b/Idh3g in TCA cycle and the glutamate dehydrogenase 1 (Glud1) enzyme in glutamine metabolism. These metabolic reactions were consistently

myeloid cell populations according to marker gene expression analysis; (D) Heatmap of the expression of the markers for each $CD8^+$ T cell subset. (E) The clustering of the $CD8^+$ T cell subsets, i.e., the exhausted $CD8^+$ T cells, memory like $CD8^+$ T cells, effector memory like $CD8^+$ T cells, naive $CD8^+$ T cells subpopulations; (F) Percent changes of the $CD8^+$ T cell subsets across the control and the Mito-ATO treatment groups; (G) The activity of the KEGG metabolism pathways were compared between Mito-ATO and control group across the anti-tumor and pro-tumor $CD45^+$ immune cell subpopulations from the mice lung tumors. The red stars mark the ten metabolism pathways whose activity changes were similar to OXPHOS activity changes by Mito-ATO treatment in these immune cell populations. The blue stars mark the four cell death-related pathways that were negatively correlated with OXPHOS activity changes by Mito-ATO treatment; (H) Under Mito-ATO treatment, the key metabolic reactions of the TCA cycle and glutamine metabolism were up-regulated across the anti-tumor immune cell populations of effector memory like $CD8^+$ T cells, memory like $CD8^+$ T cells, CD4T_Cytotoxic, and M1 macrophage cells; (I) The key metabolic reactions of the TCA cycle and glutamine metabolism were down-regulated across the immunosuppressive immune cell subpopulations of CD4IL2RALO, G-MDSC, mast cells, CD4IL2RAHI and CD4T_Exhausted cells by Mito-ATO treatment; (J) The metabolic reaction steps in TCA cycle and glutamine pathways that exhibited the 'plasticity' in reaction activity under Mito-ATO treatment between anti-tumor and pro-tumor immune cells, which involved the key enzymes of Aco1/Aco2, Mdh1/Mdh2, Idh3a/Idh3b/Idh3g in the TCA cycle and the Glud1 enzyme in the glutamine metabolism; (K) The pyruvate metabolism pathway was significantly up-regulated by Mito-ATO in the Mito-ATO-stimulated OXPHOS-high cells; (L) The pyruvate metabolism pathway was significantly down-regulated by Mito-ATO in the Mito-ATO-suppressed OXPHOS-low cells; (M) The glutamine metabolism pathway was not significantly changed by Mito-ATO in the Mito-ATO-stimulated OXPHOS-high cells; (N) The glutamine metabolism pathway was significantly down-regulated by Mito-ATO in the Mito-ATO-suppressed OXPHOS-low cells; (O) The up-regulation of the pyruvate metabolism genes by Mito-ATO in the Mito-ATO-stimulated OXPHOS-high cells and the down-regulation of these genes in the Mito-ATO-suppressed OXPHOS-low cells; (P) The up-regulation of the glutamine metabolism genes by Mito-ATO in the Mito-ATO-stimulated OXPHOS-high cells and the down-regulation of these genes in the Mito-ATO-suppressed OXPHOS-low cells; (Q) OCR analyses of vehicle- versus mito-ATO treated activated $CD8^+$ T cells in vitro; (R) ECAR analyses of vehicle- versus mito-ATO treated activated $CD8^+$ T cells in vitro; (S) OCR analyses of vehicle- versus mito-ATO treated G-MDSC cells in vitro; (T) ECAR analyses of vehicle- versus mito-ATO treated G-MDSC cells in vitro. Data are shown as the mean ± SE; n = 5-16 per group. *** $P < 0.001$; **** $P < 0.0001$. Abbreviations: Tregs, regulatory T cells; Tgd, gammadelta T cells; NK cells, natural killer cells; pDC, plasmacytoid dendritic cells; cDC, conventional dendritic cells; G-MDSC, granulocytic myeloid derived suppressor cells; CD8T_Exhausted, exhausted $CD8^+$ T cells; CD8T_MemoryLike, memory like $CD8^+$ T cells; CD8T_EffectorMemory, effector memory like $CD8^+$ T cells; CD8T_Naive, naive $CD8^+$ T cells; KEGG, Kyoto Encyclopedia of Genes and Genomes; OXPHOS, oxidative phosphorylation; Mito-ATO, mitochondria-targeted atovaquone; CD4T_Cytotoxic, cytotoxic $CD4^+$ T cells; CD4IL2RALO, IL2RA-low $CD4^+$ Treg; CD4IL2RAHI, IL2RA-high $CD4^+$ Treg; CD4T_Exhausted, exhausted $CD4^+$ T cells; TCA, tricarboxylic acid; ROS, reactive oxygen species; Aco1, aconitase 1; Aco2, aconitase 2; Mdh1, malate dehydrogenase 1; Mdh2, malate dehydrogenase 2; Idh3a, isocitrate dehydrogenase 3 alpha; Idh3b, isocitrate dehydrogenase 3 beta; Idh3g, isocitrate dehydrogenase 3 gamma; Glud1, glutamate dehydrogenase 1; FDR, false discovery rate; NES, normalized enrichment score; Ldha, lactate dehydrogenase A; Mpc2, mitochondrial pyruvate carrier 2.

up-regulated by Mito-ATO in anti-tumor immune cells but down-regulated in pro-tumor immune cells (Figure 1J).

Furthermore, we performed gene set enrichment analysis (GSEA) [7]. We combined datasets of anti-tumor immune cells, which were termed Mito-ATO-stimulated OXPHOS-high cells since their OXPHOS was enhanced by Mito-ATO treatment. Analogously, we combined the pro-tumor immune cells and named them Mito-ATO-suppressed OXPHOS-low cells. The pyruvate pathway was up-regulated by Mito-ATO in Mito-ATO-stimulated OXPHOS-high cells (false discovery rate [FDR] = 0.18, normalized enrichment score [NES] = 1.23, Figure 1K) while down-regulated in Mito-ATO-suppressed OXPHOS-low cells (FDR = 0.13, NES = -1.22) (Figure 1L). The glutamine pathway was not significantly changed by Mito-ATO in Mito-ATO-stimulated OXPHOS-high cells (FDR = 0.65, NES = -0.86, Figure 1M) but down-regulated in Mito-ATO-suppressed OXPHOS-low cells (FDR = 0.03, NES = -1.40, Figure 1N). For pyruvate metabolism, Mito-ATO treatment up-regulated lactate dehydrogenase A (Ldha), mitochondrial pyruvate carrier 2 (Mpc2), pyruvate kinase (Pkm) expression in Mito-ATO-stimulated OXPHOS-high cells while down-regulated their expression in Mito-ATO-suppressed OXPHOS-low cells (Figure 1O). For the glutamine metabolism pathway, Mito-ATO treatment up-regulated Glud1, glutamic-oxaloacetic transaminase 1 (Got1) and Mdh1 expression in Mito-ATO-stimulated OXPHOS-high cells while down-regulated their expression in Mito-ATO-suppressed OXPHOS-low cells (Figure 1P). Interestingly, Mdh1 and Glud1 were also identified by Compass analysis to be significant TCA cycle and glutamine metabolic reaction regulators (Figure 1J). Therefore, the anti-cancer efficacy of Mito-ATO treatment may be realized through differential regulation of TCA and glutamine metabolism between anti-tumor and pro-tumor immune cells, in which the expression changes of Mdh1 and Glud1 could be critical. As orthogonal validation, the Seahorse metabolic flux assay showed that Mito-ATO treatment significantly increased OXPHOS activity and aerobic glycolysis in activated $CD8^+$ T (Figure 1Q-R). In contrast, Mito-ATO significantly suppressed OXPHOS and glycolysis in G-MDSCs (Figure 1S-T). These supported the predicted higher OXPHOS and glycolysis in effector memory $CD8^+$ T cells and lower OXPHOS and glycolysis in G-MDSCs upon Mito-ATO treatment.

The metabolic plasticity of different types of cells in the tumor microenvironment (TME) in response to a glutaminase inhibitor Ethyl 2-(2-amino-4-methylpentanamido)-DON (JHU083) has been reported [8]. In the present study, we found that Mito-ATO may differentially regulate pyruvate metabolism, glutamine metabolism and TCA cycle across immune cells with distinct roles in the TME. The metabolic plasticity effects caused by Mito-ATO treatment may contribute to the overall efficacy of this drug on lung tumors. Mito-ATO's parental compound – ATO has begun to be applied to anti-cancer clinical trials [9]. Given that Mito-ATO is much more potent against human cancer cell lines compared to ATO [10], it is reasonable to predict that Mito-ATO has great potential in clinics.

DECLARATIONS AUTHOR CONTRIBUTIONS

DHX did the data analysis of this project and drafted the manuscript. ZY helped with Compass analysis. MFH did the mice experiment and scRNA-seq experiment. MH synthesized the Mito-ATO compound used in this study. YW, BK, and STW helped in preparing experimental samples and worked with MY to revise the manuscript. MY also designed this study.

ACKNOWLEDGEMENTS

This work was supported by grants from National Institutes of Health (R01CA223804, R01CA232433, R01CA205633, and R01CA280746). This work was supported in part by the International Research Project SuperO2 from CNRS, France.

CONFLICT OF INTEREST

The authors declare no conflict of Interest.

FUNDING INFORMATION

This research was supported by National Institutes of Health (NIH): R01CA223804, R01CA232433, R01CA205633, and R01CA280746.

DATA AVAILABILITY STATEMENT

The data that support the findings of this study are available from the corresponding author upon reasonable request.

ETHICS APPROVAL AND CONSENT TO PARTICIPATE

The animal study was reviewed, and all procedures were approved by the Medical College of Wisconsin (MCW) Institutional Animal Care and Use Committee (Ethics approval number of AUA00001807).

CONSENT FOR PUBLICATION

Not applicable.

Donghai Xiong[1]
Zheng Yin[2]
Mofei Huang[1]
Yian Wang[1]
Micael Hardy[3]

Balaraman Kalyanaraman[4]
Stephen T Wong[2]
Ming You[1]

[1]*Center for Cancer Prevention, Houston Methodist Neal Cancer Center, Houston Methodist Hospital, Weill Cornell Medicine, Houston, Texas, USA*
[2]*Department of Systems Medicine and Bioengineering, Houston Methodist Cancer Center, Houston Methodist Hospital, Weill Cornell Medicine, Houston, Texas, USA*
[3]*Aix Marseille Univ, Centre National de la Recherche Scientifique (CNRS), Institut de Chimie Radicalaire (ICR), Unité Mixte de Recherche (UMR) 7273, Marseille, France*
[4]*Department of Biophysics, Medical College of Wisconsin, Milwaukee, Wisconsin, USA*

Correspondence
Ming You, MD, PhD, Center for Cancer Prevention, Houston Methodist Cancer Center, Houston Methodist Research Institute, Weill Cornell College of Medicine, Houston, TX, USA.
Email: myou@houstonmethodist.org

ORCID

Ming You https://orcid.org/0009-0004-8713-9765

REFERENCES

1. Efferth T. From ancient herb to modern drug: Artemisia annua and artemisinin for cancer therapy. Semin Cancer Biol. 2017;46:65-83.
2. Huang M, Xiong D, Pan J, Zhang Q, Wang Y, Myers CR, et al. Prevention of Tumor Growth and Dissemination by In Situ Vaccination with Mitochondria-Targeted Atovaquone. Adv Sci (Weinh). 2022;9(12):e2101267.
3. Butler A, Hoffman P, Smibert P, Papalexi E, Satija R. Integrating single-cell transcriptomic data across different conditions, technologies, and species. Nat Biotechnol. 2018;36(5):411-20.
4. Carmona SJ, Siddiqui I, Bilous M, Held W, Gfeller D. Deciphering the transcriptomic landscape of tumor-infiltrating CD8 lymphocytes in B16 melanoma tumors with single-cell RNA-Seq. Oncoimmunology. 2020;9(1):1737369.
5. Oh DY, Kwek SS, Raju SS, Li T, McCarthy E, Chow E, et al. Intratumoral CD4(+) T Cells Mediate Anti-tumor Cytotoxicity in Human Bladder Cancer. Cell. 2020;181(7):1612-25 e13.
6. Wagner A, Wang C, Fessler J, DeTomaso D, Avila-Pacheco J, Kaminski J, et al. Metabolic modeling of single Th17 cells reveals regulators of autoimmunity. Cell. 2021;184(16):4168-85 e21.
7. Subramanian A, Tamayo P, Mootha VK, Mukherjee S, Ebert BL, Gillette MA, et al. Gene set enrichment analysis: a knowledge-based approach for interpreting genome-wide expression profiles. Proc Natl Acad Sci U S A. 2005;102(43):15545-50.
8. Leone RD, Zhao L, Englert JM, Sun IM, Oh MH, Sun IH, et al. Glutamine blockade induces divergent metabolic programs to overcome tumor immune evasion. Science. 2019;366(6468):1013-21.
9. Ashton TM, McKenna WG, Kunz-Schughart LA, Higgins GS. Oxidative Phosphorylation as an Emerging Target in Cancer Therapy. Clin Cancer Res. 2018;24(11):2482-90.
10. Cheng G, Hardy M, You M, Kalyanaraman B. Combining PEGylated mito-atovaquone with MCT and Krebs cycle redox inhibitors as a potential strategy to abrogate tumor cell proliferation. Sci Rep. 2022;12(1):5143.

SUPPORTING INFORMATION

Additional supporting information can be found online in the Supporting Information section at the end of this article.